Accepted Manuscript

Computers & Fluids, Volume 38, Issue 6, June 2009, Pages 1243-1257

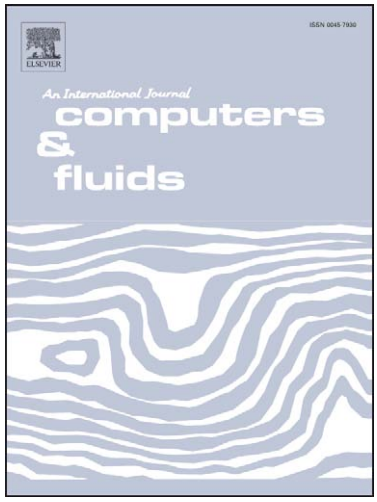

A CFD Parametric Study of Geometrical Variations on the Pressure Pulsations and Performance Characteristics of a Centrifugal Pump

R. Spence, J. Amaral-Teixeira

PII: S0045-7930(08)00233-8
DOI: 10.1016/j.compfluid.2008.11.013
Reference: CAF 1116

To appear in: *Computers & Fluids*

Received Date: 2 April 2008
Revised Date: 8 October 2008
Accepted Date: 26 November 2008

Please cite this article as: Spence, R., Amaral-Teixeira, J., A CFD Parametric Study of Geometrical Variations on the Pressure Pulsations and Performance Characteristics of a Centrifugal Pump, *Computers & Fluids* (2008), doi: 10.1016/j.compfluid.2008.11.013

A CFD Parametric Study of Geometrical Variations on the Pressure Pulsations and Performance Characteristics of a Centrifugal Pump

R. Spence[1] and J. Amaral-Teixeira[2]

[1]Clyde Pumps Limited, 149 Newlands Road, Cathcart, Glasgow G44 4EX
[2]School of Engineering, Cranfield University, Cranfield, Bedfordshire, ML43 0AL

Abstract

Pressure pulsations may be troublesome during the operation and performance of centrifugal pumps. Such pressure pulsations have traditionally been investigated experimentally but numerical analysis techniques allow these effects to be explored. The multi-block, structured grid CFD code TASCflow has been used to investigate the time variation of pressure within a complete double entry, double volute centrifugal pump. This investigation has taken the form of a parametric study covering four geometric parameters, namely the cutwater gap, vane arrangement, snubber gap and the sidewall clearance. Taguchi methods allowed the number of transient analyses to be limited to a total of twenty seven. Three flow rates were investigated and the pulsations were extracted at fifteen different locations covering important pump regions. Taguchi post-processing analysis tools were used to rank the relative importance of the four geometric parameters at each location for each flow rate. The cutwater gap and vane arrangement were found to exert the greatest influence across the various monitored locations and the flow range. A rationalisation process aimed at increased component life and reduced noise/vibration through reductions in pressure pulsations has produced geometric recommendations, which should be useful to designers.

Keywords: CFD, pump, centrifugal, parametric, pressure, pulsation.

Nomenclature

b_2	Impeller outlet width	B_3	Volute width

D_d	Discharge branch diameter
D_s	Suction branch diameter
D_2	Impeller outlet diameter
Eff	Hydraulic efficiency
n_{pj}	Number of level factor trials [n_{pj} = 3]
p	Pressure
p_j	Factor totals: Summation of the results relating to a particular factor level,
p_r*	Normalised relative pressure; $p_r^*=(p-p_1)/(\rho u_2^2/2)$
p_1	Pump suction pressure
Q_n	Nominal flow rate
R_L	Leading edge blade radius
R_1	Inlet eye radius
R_3	Radius to cutwater
t_B	Blade thickness
u_2	Circumferential speed at the impeller outlet
y_{GM}	The grand mean (average of all response values)
y_P	The predicted response
z	Blade number (per side)
β_L	Average leading edge blade angle
Δp	Peak-to-peak pressure pulsation
Δp^*	Normalised pressure pulsation; $\Delta p^*=\Delta p/(\rho u_2^2/2)$
Δ_p	Effect for factor p, where $\Delta_p=(p_1/n_{p1})-(p_{-1}/n_{p-1})$
$(\Delta_p/2)$	Half effect for factor p
θ	Total blade wrap angle
ρ	Density of the fluid

suffixes

i	1 denotes inlet 2 denotes outlet 3 denotes cutwater
j	level of Taguchi factor (-1: low, 0: mid, +1: high)
p	denotes geometric factor A: cutwater gap B: snubber gap C: sidewall clearance D: vane arrangement AB: Interaction of factors A and B

1 Introduction

Centrifugal pumps are used in a wide range of applications and they can handle a variety of liquids at relatively high pressures and/or temperatures. The present work focuses on a scaled down version of a high energy, double entry double volute pump. Double entry pumps are used in applications that would require a high flow in a single stage pump. However, due to the high energies involved these pumps tend to suffer more from pressure pulsations than single entry pumps.

A number of investigators have considered the effect of geometry modifications on the pressure variations within pumps, either by monitoring the pressure directly or through changes in the axial and/or radial thrust. Uchida et al [1] performed tests that involved monitoring the radial force and pump performance for different volute cutwater gaps and cutwater shapes using a single entry end suction pump.

In 1978, Makay and Szamody [2] reported research into the major causes of pump failure (see also Spence and Purdom [3]). They suggested that emphasis on gaining high efficiencies at design conditions led to undesirable flow features at part load operation and provided a thorough examination of pumps and pump design relating to performance difficulties. Makay and Szamody highlighted the importance of internal pump clearances, especially those between rotating and stationary parts where high gradients exist. A later report [4], which covered similar ground recommended that the safe minimum flow for a large feed pump should be 25% of the design flow condition; also that on double-entry impellers the impeller blade should be staggered (or clocked) to minimise hydraulic forces and that for double entry impellers the central shroud should be extended to the impeller outer diameter. Unfortunately, these recommendations were not presented with any back up information or discussion of the possible performance changes in the pump due to either

design modification. Sudo et al [5] provide some experimental information concerning the variation in pressure pulsations at the pump discharge due to the cutwater gap, skew of the cutwater tongue and the clocking of the impeller. Sudo et al report that the staggered impeller vanes produce pulsation amplitudes of around a quarter of those present for an inline impeller arrangement, but their measurements were some distance from the pump discharge.

It has generally been accepted that while the accuracy of CFD analyses has not yet achieved a level that is equivalent to experimental techniques, its ability to correctly predict the direction of any changes is reliable [6]. Others consider that CFD can be particularly adept in aiding understanding of the effect of ranges of parameters [7]. Yet little has been published regarding CFD being used for parametric studies, although work performed at the University of Oviedo has recently compared two impeller diameters, i.e. González-Pérez et al [8] and Blanco et al [9]. Earlier work by Spence and Teixeira [10] has shown the feasibility of generating a numerical model of a complete pump geometry and conducting CFD analyses using this model over a flow range from 1.00Qn (BEP) down to 0.25Qn. That study also compared the pressure pulsations from the numerical analysis at locations within the impeller, volute and leakage flow passages with experimental test data and reasonable agreement was found. The numerical model was also found to correctly predict pressure pulsation trends for different pump geometries. Additionally, information relating to some of the internal flow features observed within the pump both at BEP and reduced flow rates has also been published [11].

This present paper uses the analysis in [10] to provide a wider parametric study that investigates the effect of various geometry features on the pressure pulsations in the pump. A survey of literature and industrial experience provided a shortlist of key parameters in the design process and that are likely to have an effect on the pressure variation in the pump. These key areas are, the cutwater clearance gap [radial distance between impeller blade tip and the volute cutwater], the snubber

clearance gap [radial distance between the shroud outer diameter and the volute casing], sidewall clearance [minimum axial distance between the impeller shroud and the volute casing] and blade clocking or stagger [on a double entry impeller this is the practice of offsetting the arrangement of blades on one side of the impeller so that they do not coincide with the blades on the opposite side]. The parametric study utilises a Taguchi array to reduce the number of analyses required at each flow rate, with three flow rates being investigated, namely 1.00Qn, 0.50Qn and 0.25Qn. The array provides a framework for the post processing of the results and allows the reduction of the pressure pulsations in conjunction with the adjustment of the above variables. This is a rationalisation process that does not solely focus on reducing the pressure pulsation since other critical factors, such as the pump generated head, are also considered. Broadly, the objective of this rationalisation is to assist the development of pump designs, which will achieve reduced levels of pulsations without significant loss in performance.

2 Pump Geometry

The centrifugal pump simulated is of a double entry, double volute type, shown in Figure 1, with a specific speed of 0.74. The double entry impeller has a maximum diameter of 366mm, with 6 backwards curved blades per side. It should be noted that the largest impeller diameter used in the investigation was deliberately oversized for the pump design. The impeller blade has average inlet and outlet angles of 26 and 22.5 degrees respectively, with the blade wrap angle being 102 degrees. The cutwater tongue is at a diameter of 380mm, with a radius of 12mm. The pump operates at a speed of 1400rpm, with a duty flow condition of 550m3/h. The duty flow condition used in all analyses relates to the design flow rate for the original pump and so the pump will not be operating at its optimal flow condition. Table 1 provides a list of the main characteristics of the pump.

The geometrical factors considered for the parametric study are shown in Figure 2 and the values given in Table 2. Three cutwater gaps are considered, 3.83%, 6.00% and 7.95%, based on the

actual blade diameter. The change in cutwater gap was achieved by reducing the impeller blade diameter (corresponding impeller blade diameters are 366mm, 358.5mm and 352mm respectively). Three snubber gap sizes are also considered, namely 0.27%, 1.10% and 1.27%, also based on the shroud diameter, along with three sidewall leakage flow clearances that are for convenience termed 100%, 50% and 25% where 100% corresponds with a 12mm clearance in this case. Finally three different impeller arrangements are considered, an inline or straight arrangement, a mid position stagger (30 degree) and a quarter position stagger (15 degree). Figure 3 shows the different impeller arrangements. It should be noted that the staggered impeller arrangements contain a central hub extended to the outer impeller diameter, while the inline impeller terminates the hub at a radius part way through the impeller. Table 2 provides information relating to the various arrangements analysed.

3 Numerical Model

The numerical simulation is conducted using CFX-TASCflow, which utilises a finite element based finite volume method to solve the unsteady three-dimensional Navier-Stoker equations on a structured grid. CFX-TASCflow also has the advantages of including some turbomachinery specific capabilities at the pre- and post- stages of the simulation.

As has been noted earlier, a previous paper [10] contains detailed information concerning the generation of the numerical model. This previous paper includes descriptions of the grid independence checks conducted, in addition to the examination of different boundary conditions and turbulence models with a view to achieving a robust analysis in a reasonable timeframe while preserving the accuracy of the analyses. Information relating to the interpretation of the data gained from the analyses and comparisons with industrial experimental tests are also provided in this previous work. A brief summary of this work is contained below.

3.1 Grid Generation

The pump is split into a number of component parts for modelling. The component parts included, (a) the double suction inlet, (b) the leakage flow paths comprising the snubber gap, sidewall clearance and wear ring gaps, (c) the pump impeller (both sides), (d) the double volute and (e) a mid block between the two sides of the impeller (the mid block is only present for staggered impeller arrangements). Due to the size and complexity of the pump care was taken regarding the distribution of grid elements in the model. A detailed grid independence check was conducted for the impeller grid using single passageway sizes ranging from 10000 to 85000 elements, with the influence of the volute on the flow in the impeller grid being factored into the check. This concluded that an impeller grid size of 22000 elements/nodes per passageway was sufficient to reliably model the pressure in the impeller. The impeller model consisted of 12 passageways and totalled 227126 elements. Care was taken to concentrate grid in the cutwater region of the volute and the axial distribution at the impeller interface replicated the impeller grid distribution. In total, 391848 elements were used to model the volute. The leakage flow path model was generated in such a way that multiple snubber and sidewall geometric arrangements could be analysed through use of a single grid and the block-off feature in CFX-TASCflow. The leakage flow path comprised 161760 grid elements. The suction inlet model consisted of 89756 elements. The model was assembled using a step-by-step iterative process that allowed each component grid model to be examined and refined in order to improve the interaction of the flow between components. This was a time consuming process, but gives confidence in the large, complex numerical model since each component was capable of modelling not only its internal flow satisfactorily, but had also been generated with consideration of interactive effects with other components. Once complete the total pump model consisted of 870500 hexahedral elements. Figure 4 provides an indication of the overall model mesh.

3.2 Pre-Processing

The pre-processing set up of the pump model was conducted with consideration of the limitations involved with gaining a stable transient analysis while performing analyses over a wide range of flow conditions. The impeller and leakage flow grid components were set in a rotating frame of reference. The interfaces between rotating and stationary frames were modelled using the rotor/stator interface option; interfaces between components in the same frame of reference use the general grid interface (GGI) option. Although a number of boundary conditions were examined, the parametric study was conducted using a mass flow at inlet and static pressure at outlet as this set of boundary conditions had been found to be more stable and converge faster than other combinations without a significant loss in accuracy. As noted above the duty flow condition for all geometry configurations was 550 m3/h. This decision was made to ensure consistency with experimental work that was conducted with a single duty flow rate. The flow rates chosen for examination in this project were deliberately selected at significant spacing to preserve general trends with varying flow rate. It was calculated that the extremes of geometry would indicate a best efficiency point shift of less than 5% in the flow rate. The internal and external impeller surfaces were modelled using a rotating wall, while all other walls were stationary.

Turbulence was modelled with a standard k-epsilon model; wall functions based on the logarithmic law were used. A second order discretisation process was employed in the transient analyses. The calculations were conducted serially on computers that contain two Intel 3GHz processors with 6GB of shared memory apiece. The time taken per iteration is dependent on the arrangement and flowrate analysed, but is approximately one iteration per hour. Typically periodic unsteady convergence was achieved in four to five impeller revolutions. The timestep selected for use in the current analyses was 1.488·10-4 seconds, as this provided 288 time steps per impeller rotation (48 time steps per blade passage). This timestep was chosen based upon the work of Koumoutsos [12] who conducted transient analyses of a centrifugal pump using time steps equivalent to 250 and 500 time steps per revolution and concluded that 250 time steps per revolution (50 time steps per

revolution) was adequate for a reliable and accurate analysis. Thus the selection of the timestep, giving a greater number of time steps per impeller revolution, was considered to have preserved the accuracy and stability of the analysis, with the Courant Freidrich Levy (CFL) number being less than 30. Transient results files were created after every second iterative loop.

3.3 Pressure Pulsation Monitoring Locations

The pressure pulsation level was investigated at fifteen locations around the pump. Figure 5 provides the circumferential position of a number of the locations in the volute and leakage flow passage.

Leakage Flow Locations (in casing wall in leakage flow path at back of impeller)

C1 – 60mm ahead of the leading edge cutwater (not shown)

C2 – 30mm ahead of the leading edge cutwater

C3 – at the leading edge cutwater

C4 – 30mm past the leading edge cutwater

C10 – 60mm ahead of the leading edge cutwater, opposite to C1 (not shown)

Volute Locations (at splitter, 25mm axially offset from pump centreline)

C5 – 5mm back from the cutwater leading edge

C6 – 15mm back from the cutwater leading edge

C7 – 30mm back from the cutwater leading edge

C8 – 50mm back from the cutwater leading edge

C9 – Top, centre of the pump (not shown)

Cd – Pump discharge (not shown)

Impeller Positions (all not shown)

Shroud B (above blade) – shroud outer diameter, positioned above an impeller blade.

Shroud M (mid passage) – shroud outer diameter, positioned mid way between two impeller blades.

Blade P – located on the pressure face of an impeller blade at the trailing edge.

Blade S – located on the suction face of an impeller blade at the trailing edge.

In order to keep the presentation manageable the results given in this paper are restricted to a single monitoring position in each of the major pump regions, e.g. C4 for leakage flow path, C6 for volute cutwater, C9 for general volute/towards discharge and Blade P for the impeller outlet. Results at some of the other positions will be mentioned in discussion.

3.4 Summary of Experimental Comparison

The uncertainty in the present analysis has been minimised and assessed through two approaches. Firstly through convergence studies as described in section 3.1 and by comparison with industrial based experiments. The former have shown that the present mesh size, for the impeller, is within 3% of a much finer grid. The latter is described in detail in references [10] & [11] but the results are summarised here for convenience.

Table 3 provides a comparison of the CFD simulation (arrangement 2) with experimental data for the 0.25Qn and 1.00Qn flow rates. The table gives an indication of the percentage variation of the CFD simulation with the industrial test results at a selection of locations around the pump (with the difference being divided by the experimental value). The agreement at the impeller shroud where the pulsation levels are relatively high is excellent and typically the differences are significantly lower for all flow rates than the average, being as low as 7%. It should be pointed out that the C5 and C6 positions (which show a higher difference) are very sensitive to the actual monitored location because of the high pressure pulsation gradients in the vicinity of the cutwater tongue. The shroud and C9 (towards the discharge) positions are important locations for monitoring within the

pump as the estimation of fatigue levels in the impeller requires information at the impeller shroud and the C9 position can be used to provide a more general indication of pressure pulsations within the pump. At these locations the variations are better than average and can reach levels as low as 3%. Generally within the pump, the differences have an average value across all locations being between 25%-30%, but it is important to note that all of these comparisons show substantial improvement over previous pulsation work performed by Longatte and Kueny [13] and Talha [14] who respectively reported over prediction of pulsations by 1000% and 300% in comparison with experimental tests.

In general the relationship between the numerical simulation and experimental test is rather complex. The percentage variation with the experimental values does not appear to show any identifiable improvement at flow rates closer to the BEP flow condition. However the pulsation variation at 1.00Qn is approximately half that calculated for 0.25Qn for both arrangements when averaged across all measured locations. Unfortunately only limited experimental performance data is available for comparison, i.e. no efficiency information was recorded. However, for the arrangement shown, the comparison of the available data indicates that the CFD simulation predicts the pump generated head to within 4% of the experiment at the 1.00Qn flow rate, with this increasing to 7% at the lowest flow condition.

3.5 Presentation and Discussion of Results

The output from the CFD analyses provided a time history of the pressure variation and performance characteristics as the impeller rotated in the volute. Figure 6 provides sample time histories of the normalised relative pressure at the four selected locations around the pump for the fifth geometrical arrangement (shown in Table 2) and at 1.00Qn. The relation of the pressure pulsation to the movement of the blade relative to the cutwater can be described using Figure 6a (i.e. a location at the cutwater). The highest pressure, occurring at zero degrees and every 60

degrees thereafter, takes place just before the pressure face of the impeller blade reaches the cutwater. As the blade passes the cutwater the effect of the wake impinging on the cutwater causes a sharp decrease in the pressure, with a minimum being reached as the suction face of the impeller blade passes the cutwater. Then, as the impeller blade continues past the cutwater the pressure rises rapidly. The time period for this pulsation in pressure is short, relating to under half the time for each blade pass. The C4 position (in the leakage flow passageway), Figure 6(b) records a regular pulsation with the pulsation frequency corresponding to blade rate. The amplitude of pulsation is generally half that experienced at the cutwater. Figure 6(c) illustrates that the pulsations at C9 (approaching the outlet) are approximately a quarter of those recorded at the cutwater; the location does identify the peaks corresponding with the blade passing frequency. The impeller blade pressure face location time history, Figure 6d, shows two larger peaks corresponding to the blade passing the splitter (180 degrees) and the cutwater (zero/360 degrees) respectively. It can be observed that although the splitter and cutwater have been designed to be as alike as possible, the pulsation at the splitter is significantly larger. There is also significant difference in the pressure variation from the cutwater to splitter (0-180º) than from the splitter to the cutwater (180-360º). The positive pressure gradient in the initial half of the casing is likely due to the use of an oversize impeller in the analyses indicating that the 1.00Qn flow condition is actually lower than the optimum design flow rate. This indicates that slight differences in each half of the volute geometry results in them having different optimised flow conditions.

It should be noted that although peak-to-peak pulsations are investigated for each location, the purpose of the investigation is to gain an indication of the change (and rate of change) of these maxima with differing geometries rather than identify the location of the highest pressure pulsation within the pump. In order to present the parametric results in a concise fashion, the maximum peak-to-peak pressure pulsations results for all nine arrangements and the three flow rates have been extracted from graphs similar to Figure 6. These are presented in Tables 4, 5 and 6 respectively.

It is clear that the pressure pulsations increase as the flow decreases and that the largest pulsations exist at the trailing edge of the impeller blade. The pulsations at the volute cutwater are larger than those in the leakage region and the cutwater gap and vane arrangement are the geometric parameters with the strongest effects.

4 Taguchi Background

Taguchi's concept was to design a quality product rather than inspecting a product to determine if it was a quality product. The Taguchi methodology optimises the configurations used in a parametric study such that fewer configurations are required to identify the relative importance of the selected parameters. The Taguchi approach sets out configurations (or arrangements) to be conducted using an appropriate orthogonal array; the terminology used in these arrays includes "factors" – an item that is to be varied during the simulations, "level" – the number of times a factor is to be varied during the simulations and "configuration number" - the number of simulations that are required to be run to complete the analysis. Thus the cutwater gap is a "factor", which has three levels (i.e. 3.83%, 6.00% and 7.95%). In total, the simulations conducted in this work are to investigate four, three level factors (i.e. cutwater gap, snubber gap, sidewall clearance and vane arrangement).

The selection of an appropriate Taguchi array is dependent on the number of factors and the levels of the factors to be analysed. The letter L and a subscript number identify the arrays. Roy [15] provides a table of common orthogonal arrays and their related number of factors and levels, which indicates that for the current requirement the L_9 array is appropriate. To produce a full factorial parameter study of the geometric variables, the number of cases required would be 243 (4 factors with 3 levels at 3 flow rates). The Taguchi approach reduces this to 27 cases. The layout of the L_9 array with the various factors and levels is shown in Table 2. It was considered that an L_4 array with two factors and two levels could be used to provide additional information for the significant

factors from the L_9 array. Two L_4 arrays have been used and these are shown in Tables 4 and 5, consisting of arrangements previously analysed as part of the larger L_9 array. The particular arrangements used to form the smaller L_4 arrays depend on the results of the L_9 array.

Pressure pulsations have been used as the quality characteristic, with “the lower the better” being set as the criterion of evaluation. Other quality characteristics such as the pump performance (e.g. the pump generated head, or hydraulic efficiency [calculated between the pump suction and discharge]) could also be selected with its own criterion of evaluation. The analysis conducted on the L_9 array result data is essentially an analysis of variance (ANOVA) as detailed in Roy [15].

5 Taguchi Post-Processing of Results

5.1 Response Averages

One aspect of the Taguchi method utilises response averages, calculated for each location and flow rate in relation to a specific geometry parameter variable, to provide detail relating to the influence of the geometric factors on the pulsations (and generated head). For example, to calculate the response average at location C6 relating to the 3.83% cutwater gap at 1.00Qn, the average of the C6 pressure pulsations would be calculated from arrangements 1, 2 and 3. The Taguchi method splits each of the four geometrical parameter variables into their "levels", termed high [+1], mid [0] and low [-1]; the relation of these levels to the geometrical variables is shown in Table 2. Sample calculated response average values for each level and for all parameters are shown for the C6 location in Table 7 for the duty flow condition. These averages are provided for a selection of locations across the three flow rates in Figures 7 and 8 showing the effect of the cutwater gap and vane arrangement respectively. Due to the discrete geometry changes involved the vane arrangement graphs are simply joined with straight lines rather than curves. It should also be noted that the scale for Figure 7d and 8d (both blade pressure locations) is double that used at the other locations. These graphs together with the general pulsation and performance data provide detail

relating to the influence of the dominant geometric parameters mentioned above (vane arrangement and cutwater gap). The influence of the cutwater gap is most significant at the impeller outlet and at circumferential positions close to the cutwater. It should be noted that for location C6 (Figure 7b) that there is a slight reduction in the rate of pulsation reduction as the cutwater increases at 1.00Qn and 0.25Qn flow rates. Figure 9a illustrates the strong influence of the cutwater diameter on the generated head, with the head decreasing as the cutwater gap increases (the power graph, not shown, shows similar trends). The reduction in head and power are as a direct effect of the cutwater gap being modified by changing the impeller outlet diameter. Pump scaling laws predict that the head will reduce with the square of the impeller diameter. The vane arrangement has an effect on the pulsations at most of the monitored locations. Typically the inline vane arrangement has larger pulsations than either of the two staggered vane arrangements, with the 15 degrees vane arrangement being closer to the 30 degrees vane results rather than the inline arrangement. The vane arrangement has the strongest effect on the pressure pulsations at the leakage flow and volute locations that are remote from the cutwater position. Reductions in the pressure pulsations local to the cutwater (shown clearly at C6, Figure 8b) and the impeller blade pressure face location, Figure 8d, due to the vane arrangement are generally less than reductions due to the cutwater gap increase. On some occasions the 15 degree stagger vane produces lower pulsations, yet at others the 30 degree stagger vane arrangement is lower. Figure 9b illustrates that the vane arrangement has a small but noticeable influence on the performance characteristics, with the head and power (not shown) reducing slightly when moving from an inline arrangement to a staggered arrangement. It is possible that the reduction in the generated head is caused by additional friction loss present due to the central hub extending to the outlet in the staggered case instead of terminating earlier in the inline arrangement. The pump hydraulic efficiency is generally larger for a staggered impeller arrangement than an inline vane arrangement.

5.2 Percentage Contributions

One other important aspect of the Taguchi method is the ability to calculate the percentage contribution of a geometric parameter to a specified quality characteristic. The percentage contributions are calculated from an analysis of variance that effectively measures how far the pulsation values for a specific geometry variable vary from the mean. The amount that the high and low parameter levels vary from the mean provides a measure of that parameter's influence on a particular quality characteristic. This is converted in to a percentage value to provide a measure of the contribution relative to the other parameters. Again percentage contributions have been calculated for each specific location and for all flow rates. A summary of the contributions for the three flow conditions, at the same locations as earlier, is provided in Tables 8 to 10 for flow rates 1.00Qn, 0.50Qn and 0.25Qn respectively. The percentage contributions provide a great deal of information regarding the importance of the various geometric factors and it is interesting to observe how at some locations the trends are consistent across the flow range, while other locations experience significant variations.

In the leakage flow passageway the vane arrangement is the dominant parameter although this dominance reduces as the flow rate reduces, especially in locations circumferentially close to the cutwater. The cutwater gap shows a lesser contribution, however this increases as the flow rate decreases and for locations circumferentially close to the cutwater. The snubber gap and sidewall clearance generally have a significantly lesser effect, although this can become more significant at lower flow rates. In the volute, the cutwater is the controlling parameter for pulsations close to the cutwater, with this influence decreasing significantly the greater the distance from the cutwater (i.e. down to 16% at C9 for 1.00Qn). The vane arrangement shows the opposite trend, with its percentage contributions being around 30% close to the cutwater and increasing to 80% prior to the splitter. The trends in pulsation in the volute are relatively consistent across the flow range examined, with the exception that snubber and sidewall clearances have an increased influence at

the lower flow rates. At the impeller trailing edge the cutwater gap is effectively the sole parameter effecting the pressure pulsation at the duty flow condition and although reduces at lower flows continues to be dominant. The vane arrangement shows an increasing influence as the flow reduces, with the snubber gap and sidewall varying in importance depending on the flow rate. In relation to the performance characteristic, the cutwater gap exhibits the largest contribution to the pump generated head at all flows (this contribution is around 90% at all flow rates). The power characteristic is again dominated by the cutwater gap, especially at the higher flow rates, with the vane arrangement being of secondary importance. It is interesting to note that while the head and power contributions for the vane arrangement are relatively low, the contribution to the hydraulic efficiency at 1.00Qn and 0.50Qn is surprisingly large.

5.3 Interactive Effects and Predictive Equations

The L_9 array provides useful information in the form of the percentage contributions, but does not provide information on interaction effects between the geometric parameters. Of the four factors investigated, the cutwater gap and the vane arrangement are the two most important by a significant degree. An L_4 Taguchi array can now be used to gauge the interactive effect between these two factors. The investigation was performed in two stages. For the first stage, a single array was formed for each flow rate, with the vane arrangement being limited to either being inline or with a 30 degree stagger and the cutwater being variable between 3.83% and 7.95%. Predictive equations can be generated, general form shown by Equation 1 (Schmidt and Launsby [16]), which can gauge the effect of the cutwater gap for both inline and staggered vanes. The second stage array was formed for each flow rate, for cutwater gap values of 3.83% and 7.95% and vane arrangements of 15 and 30 degree stagger. This array generated further equations that can be used to investigate the relationship between the pulsation at specific pump locations and the pump geometry.

$$y_P = y_{GM} + \left(\frac{\Delta_A}{2}\right) \times A + \left(\frac{\Delta_B}{2}\right) \times B + \left(\frac{\Delta_{AB}}{2}\right) \times AB \qquad \text{Equation 1}$$

(a) Stage 1 (Vane: Inline & 30^o Stagger, Cutwater Gap Values: 3.83% & 7.95%): The array used for stage 1 is indicated in Table 11. The interaction between the cutwater gap and the vane arrangement is investigated through representing the response averages in graphical form. Figure 10 provides an interaction plot at the 1.00Qn flow condition for a selection of locations within the pump. Parallel lines indicate little or no interaction, whereas lines with very different gradients indicate an interactive relationship between the parameters being studied. Thus, interaction does exist between the two factors examined, but not at every location. The interaction appears strongest close to the trailing edge of the impeller and almost non-existent at location C6. Similar plots (not shown) are produced for the other flow rates; these indicate that as the flow rate reduces the strength of the interactive effect can change significantly depending on the location. Table 12 provides a list of the calculated response averages, half effects ($\Delta 2$) and grand mean values for a selection of pump locations for 1.00Qn and 0.25Qn flow conditions, inclusive of the interactive effect. A comparison of the half effects shows that while the most important factor can switch between the cutwater gap and the vane arrangement, the interaction effects are never the most important and at positions away from the impeller are generally the least influential factor.

From the above information predictive equations can be generated to estimate the pressure pulsation at any of the reported pump locations, by inserting the grand mean and the half effect values for each of the factors in Equation 1. However, as only two levels are used in the L4 array to form the equation the relationship between the pulsation at a location and the geometric parameter is assumed linear. Equation 2 illustrates a sample equation for location C6 at 1.00Qn.

$$y = 0.180 - 0.054A - 0.026B - 0.001AB \qquad \text{Equation 2}$$

By varying each of the factors between –1 and 1 it is possible to determine what pressure pulsation is likely to be obtained with a certain geometry set, even if it is not one of the arrangements that was analysed. For instance, for a cutwater gap of 5% (a cutwater gap (A) factor of approximately –0.5) and an inline vane arrangement (a vane arrangement (B) factor of -1), Equation 2 predicts a

normalised pressure pulsation of 0.232 at location C6 for 1.00Qn. Similarly a 30 degree staggered impeller (a vane arrangement factor of +1), Equation 2 predicts a value of 0.180. Both of these predicted values seem sensible when compared with the analysis data contained in Table 4. Due to the marked differences between inline and staggered arrangements the vane arrangement factor is restricted to either –1 or +1, as intermediate increments will not provide realistic predictions. The Stage 2 provides a better comparison of varying the vane stagger angle.

(b) Stage 2 (Vane 15degree & 30degree stagger, Cutwater Gap Values: 3.83% & 7.95%): The array for use in stage 2 is provided in Table 13. It is not felt that there is a need to present the interaction plots similar to Stage 1, but it is worth noting that the interaction effects continue to be included. The calculated response averages and half effects are provided in Table 14 for the same pump locations shown in Stage 1. The grand mean has again been calculated and reported in this table for each pump location. Comparing the half effects indicates that, when considering all locations and both flow rates, the cutwater gap has the strongest influence. The vane arrangement (in this instance relating to the amount of stagger only) is strongest at location C9 for 1.00Qn with larger effects being present in the leakage flow region at the lower flow rate. The interactive effect is again smaller than the other two factors, however it can be seen that at location C4, it can provide a significant contribution. The data in Table 14 can be used to generate predictive equations for the pressure pulsation (or generated head) at any of the pump locations, for example Equation 3 is given for location C6 at 1.00Qn.

$$y = 0.150 - 0.053A + 0.002B - 0.001AB \qquad \text{Equation 3}$$

Again we can use this equation to predict other geometrical arrangements. For example, a cutwater gap of 5% (cutwater gap factor of approximately –0.5), and a 25 degree vane stagger angle (vane arrangement factor of around +0.33) results in a normalised pressure pulsation value of 0.178 at position C6. This could be compared, for example, with a 20 degree vane stagger angle (-0.33 vane arrangement factor), which results in a normalised pulsation of 0.176.

6 Rationalisation Leading to a Recommended Design

Design recommendations, in the present context are rather complicated, as one cannot easily optimise on "pressure pulsations" due to the complex relationships between geometry and pressure pulsations that vary with the location in the pump and flow rate. Thus a rationalisation process is adopted. In the present context it is important to reduce pulsations for two main reasons, firstly to avoid fatigue damage and extend the life of pump components and secondly to reduce the vibration levels due to hydraulic effects. A typical fatigue failure of an impeller shroud is shown in Figure 11, where a section of the shroud has been torn away by the pressures exerted on it. The aim would be to increase component life by reducing the pressure pulsations at the impeller outlet. Large pulsations in the pump cause vibration and noise and the aim would be to reduce hydraulically generated noise and vibration by reducing the overall level of pressure pulsations in the pump. These requirements could exist separately or together depending on the application. Additionally, regardless of the motivation behind the process, the benefit gained in terms of pulsation reduction must be balanced against any possible loss in pump performance.

6.1 Consideration of Component Life

The usual initial step in extending component life, where fatigue is a factor, is to minimise any stress concentration factors present in the component. However the stress concentrations in some important areas, e.g. where the impeller blade connects to the shroud, have limited potential for improvement. Therefore, with the detailed mechanical design constrained by the impeller dimensions, it is important to minimise the hydraulic pressure loadings and fluctuations on the impeller. It is possible by rational argument to arrive at an improved design through considering each geometric factor and its effect.

The cutwater gap exerts one of the strongest influences on the pulsations at the impeller outlet. Although only the blade pressure face results have been shown, this section will also utilise results for the shroud monitoring locations. The change in pulsation at the blade pressure face, Figure 7(d), shows a slight non-linearity at lower flow rates, this non-linearity is more pronounced at the shroud locations (not shown) indicating that as the cutwater is increased the rate of pressure pulsation reduction reduces. The relationship between the generated head and the cutwater gap, Figure 9(a) is linear at all flow rates with a slight non-linearity at the lowest flow condition. Thus any increase in the cutwater gap will reduce the pressure pulsation, but this must be tempered by the reduction in head. However, the non-linearity of the shroud pulsations, especially at lower flow conditions, indicates a lesser reduction in pulsations at this location as the cutwater gap increases. Therefore a cutwater gap of around 6% or slightly larger provides a substantial reduction at both the blade and shroud locations. Increasing the cutwater gap above 6% will provide a lower amount of pulsation reduction at the shroud for a continuing reduction in head.

The vane arrangement has a mixed effect on the pressure pulsations at the impeller outlet. Figure 8(d) shows that the staggered arrangement appears to decrease the pulsations at the impeller blade tip at all flow rates (with the exception of the 30 degree stagger at the lowest flow condition). At shroud locations (not shown), both staggered arrangements provide significant pulsation reductions in comparison to the inline blade impeller. Figure 9(b) indicates that while a staggered impeller will reduce the generated head, the 15 degree stagger involves a greater reduction that the 30 degree stagger. As the failure mechanism for impellers is focused at the impeller vane/shroud connection caused by pressure across the shroud span at outlet, it is judged that reduction of pressure variation at the impeller outlet is of significant importance when considering the life of the impeller. On this basis a staggered impeller is a better option than the inline impeller. However there is some uncertainty whether the 30 degree stagger should be preferred over the 15 degree arrangement.

It is considered that a tight snubber gap will prevent the pulsation from passing into the leakage flow area; causing the pulsation energy to remain close to the impeller outlet. Conversely, a large snubber gap allows the pulsation to pass into the leakage flow region causing large shifts in pressure, which can cause shuttling if the gap is sufficiently large [17]. Therefore some mid size snubber gap that is large enough to allow the pulsation to pass away from the impeller tip into the leakage path, yet not enough to cause the shuttling effect is required. In industry, a general rule of thumb relating to the snubber gap is that the length of the snubber gap should be approximately six times its height in order to attenuate the pressure pulsations. The shroud thickness for the analysed impeller is 7mm, indicating that the "maximum" snubber gap according to these rules would be 0.64% (3mm in this study). As the snubber gap can cause some reduction in pulsation at the lower flow rates, it is recommended that the snubber gap be calculated using the 0.64% figure and rounded up to the nearest millimetre.

The sidewall clearance exhibits only a small effect on the pulsation at the impeller outlet region, and any contribution occurs at the lower flow conditions. Thus, while the sidewall clearance has no apparent effect on the performance of the pump, results indicate that maintaining a 100% clearance gap (12mm for this study) may provide slight benefits at lower flows.

6.2 Pump Noise and Vibration Levels

The pump noise and vibration levels due to blade passing frequency relates directly to general pulsation levels within the pump. Published literature by Srivastav et al [18] has noted that the blade passing frequency dominates the vibration spectra and governs the overall vibration level, with the strength of the frequency being dependent on the radial gap. These unsteady interactions are also related to the radial force due to an imbalance in the pressure field at the impeller outlet, which is a cause of pump vibration. Therefore, both the vibration and acoustic levels can be related in some manner to the general variation in pressure within in the pump.

The influence of the cutwater gap is largest close to the cutwater, but its influence reduces significantly over a relatively small distance. The response averages plotted in Figure 7(a), (C6), indicate that there is a greater reduction in the pulsation in these regions up to a cutwater gap of 6.00% than for larger gap values, for a similar reduction in head. Location C9, Figure 7(c) indicates that away from the cutwater there is a lesser effect with a similar trend to that shown at locations C4 and C6. Thus, 6.00% appears to provide a substantial pressure pulsation reduction in the pump while limiting the reduction in the generated head.

A staggered impeller provides significant reductions in pulsation at most locations in the volute, especially those that are circumferentially distant from the cutwater. Both staggered vane arrangements provide significant benefits over the inline arrangement at 1.00Qn and 0.50Qn and in some cases 15 degrees is better than 30 degrees. Figure 9(b) indicates that a 30 degree stagger generates a consistently higher head than the 15 degree arrangement. This is unexpected as general opinion in industry considers that a mid position stagger forces the jet flow from one side of the impeller to mix with wake flow on the opposite side resulting in relatively high mixing losses. A plot of the axial movement of fluid (i.e. mixing) over a 2D annular area at the impeller outlet is plotted in Figure 12 for the 30 degree and 15 degree stagger angles respectively (impeller blade positions are shown). It is immediately apparent that the 30 degree vane stagger arrangement (Figure 12a) includes axial mixing of the flow over a considerably larger area than the 15 degree stagger (Figure 12b), where a higher level of mixing is indicated by a darker region. However, this larger mixing region does not appear to have had a significant effect on the pump generated head, although for other impeller designs this may not be the case. This is can likely be attributed to the 30 degree arrangement allowing a large amount of diffusion as the flow exits the impeller resulting in a lower fluctuation in flow rate. Therefore, in this case a 30 degree vane arrangement is recommended but this cannot be a universal recommendation.

Both the snubber gap and sidewall clearance parameters have small effect on the pulsation according to the percentage contributions. Therefore, for noise and vibration considerations neither parameter contributes significantly for the sizes analysed

6.3 Final recommendations

Although the pump geometry has been examined using two different motivations there is some agreement between the two. Consideration of the two rationalised arrangements allows a final "optimised" or recommended arrangement to be selected,

- The minimum cutwater gap should be 6% of the impeller diameter (11mm in this study)
- The vane arrangement should use a 30-degree stagger (i.e. a mid position stagger).
- The diametral snubber gap should be approximately 0.64% of the impeller diameter, rounded to the nearest millimetre (3mm in this study).
- The sidewall clearance should be 100% (12mm in this study).

7 Conclusions

A numerical model of an entire double entry, double volute centrifugal pump has been used to conduct a parametric study covering four main geometric parameters. The parameters include the cutwater gap, vane arrangement, snubber gap and sidewall clearance, with three different configurations being used for each parameter. A total of thirty three transient analyses have been conducted, representing 45000 hours of continual analysis time and consisting of over 550 gigabytes of analysis and result data. The pressure levels predicted by the numerical analysis give rise to an enormous and interesting data set. The results have been presented by concentrating on selected locations around the pump.

An L_9 Taguchi array has been successfully constructed for fifteen pressure monitoring locations and three performance characteristics. The analysis of the array identified the dominant geometrical influences on the pulsations and the performance of the pump. In general, the cutwater gap and vane arrangement are the two strongest influences on the pressure pulsation, with the snubber gap and sidewall clearance being considerably less important. Detailed information has been presented on pressure pulsations and performance characteristics both in terms of non-dimensional values and percentage contributions, which will assist understanding of the pump behaviour and the effect of the geometric variables.

Smaller L_4 Taguchi arrays have been employed to determine the importance of the interactive effect between the cutwater gap and vane arrangement. The interactive effect can be more important than the parameter of secondary importance, but is never as large as the dominant parameter. Basic information has been presented, which allows predictive equations to be obtained that can identify expected pressure pulsations at specific pump locations for arrangements different from those analysed. The equations are limited to linear relationships and are bounded by the maximum and minimum values used for the relevant geometric parameters used in the analyses.

The pressure pulsation information has been used with a view to firstly, increasing the component life and secondly, reduce the noise and vibration. This has been achieved through a rationalisation process and geometric recommendations have been derived that satisfy both requirements. These guidelines should be useful to designers.

Acknowledgements

This work was supported throughout by Clyde Pumps Limited and Cranfield University.

References

[1.] Uchida, N., Inaichi, K and Shirai, T. (1971). "Radial Force on the Impeller of a Centrifugal Pump." Bulletin of the Japan Society of Mechanical Engineers, 1971,Vol. 14, pp.1106-1117.

[2.] Makay, E. and Szamody O. (1978). "Survey of Feed Pump Outages." Prepared for Electric Power Research Institute Research, Project 641. Report: FR-754.

[3.] Spence, R. and Purdom, T. (1999), "Prediction of Impeller Loadings using CFD Analysis Techniques". Presented at IMechE Seminar, Up and Coming in Fluid Machinery, 17th November 1999 IMechE, London

[4.] Makay, E. and Szamody, O. (1980). "Recommended Design Guidelines for Feedwater Pump in Large Power Generating Units" (1980), Prepared for Electric Power Research Institute Research, Project 1266-18, Report: CS-1512.

[5.] Sudo, S., Komatsu, T., and Kondo, M. (1980). "Pumping Plant Noise Reduction: Reduction of Pressure Pulsation in Pump Discharge Pipe Systems." Hitachi Review vol. 29 (1930), No. 5.

[6.] Gallimore, S. (1998). "Axial Flow Compressor Design" Presented at "The Successful Exploitation of CFD in Turbomachinery Design." At IMechE, 1 Birdcage Walk, London on the 19th March 1998.

[7.] Denton, J. and Dawes, W. (1998), " CFD for Turbomachinery Design." Presented at IMechE seminar "The Successful Exploitation of CFD in Turbomachinery Design." on 19th March 1998 London.

[8.] González-Pérez, J., Parrondo, J., Santolaria, C. and Blanco E. (2006). "Steady and Unsteady Radial Forces for a Centrifugal Pump with Impeller to Tongue Gap Variation." ASME Journal of Fluids Engineering, May 2006, Vol. 128. pp. 454-462.

[9.] Blanco, E., Parrondo, J. L., Barrio, R., González, J., Santolaria, C., and Fernández J. (2006) "Fluid-Dynamic Radial Forces at the Blade-Passing Frequency in a Centrifugal Pump with

Different Impeller Diameters." IAHR international Meeting of the Work Group on Cavitation and Dynamic Problems in Hydraulic Machinery and Systems, 28-30 June 2006, Barcelona, Spain.

[10.] Spence, R.R.G and Teixeira J.A (2008). "Investigation into Pressure Pulsations in a Centrifugal Pump by Numerical and Experimental Methods." Journal of Computers and Fluids Vol 37 (2008) pp 690-704

[11.] Spence, R.R.G and Teixeira J.A (2007). "A CFD Analysis of a Complete Double Entry Centrifugal Pump" Proceedings of the 15th Annual meeting of the Association of Computational Mechanics in Engineering – UK. Glasgow, 2-3rd April 2007.

[12.] Koumoutsos, A. (1999), "Unsteady Flow Interactions in Centrifugal Turbomachinery Configurations." (Unpublished PhD Thesis) Cranfield University, Cranfield.

[13.] Longatte, F., Kueny, J.L., (1999), "Analysis of Rotor-Stator-Circuit Interactions in a Centrifugal Pump", ASME paper FEDSM99-6866.

[14.] Talha, A. (1996). "Etude hydroacoustique d'une pompe centrifuge et de son circuit immédiat par l'analyse expérimentale des pressions et des vitesse instationnaires", PhD Thesis, Université de Lille. Cited in: Longatte, F., Kueny, J.L., (1999), "Analysis of Rotor-Stator-Circuit Interactions in a Centrifugal Pump", ASME paper FEDSM99-6866.

[15.] Roy, R. (1990). "A Primer on the Taguchi Method.", Van Nostrand Reinhold, New York.

[16.] Schmidt, S. and Launsby, R. (2005). "Understanding Industrial Designed Experiments" 4th Edition, Air Academy Press, Colorado Springs.

[17.] Makay, E. and Nass, D. (1982). "Gap-Narrowing Rings Make Booster Pumps quiet at Low Flow." Power, September, pp. 87-88.

[18.] Srivastav, O. P., Pandu, K. R. M. Gupta, K. (2003). "Effect of Radial Gap between Impeller and Diffuser on Vibration and Noise in a Centrifugal Pump." Institute of Mechanical Engineers (India). Technical journal – Mechanical Engineering, MC1 – April 2003, Vol. 84, pp. 36-39.

Figure Captions

Figure 1: Pump type with horizontal cross section

Figure 2: Geometric factor locations within the pump

Figure 3: Different impeller arrangements: left to right - inline, 15 degree and 30 degree arrangements

Figure 4: Total pump grid model

Figure 5: Sketch of the circumferential position of the volute cutwater (C5, C6, C7 and C8) and sidewall (C2, C3 and C4) monitoring locations

Figure 6: Time history of pressure variation at selected locations for arrangement 5 at 1.00Qn

Figure 7: Cutwater Gap normalised response averaged pressure pulsations

Figure 8: Vane Arrangement normalised response averaged pressure pulsations

Figure 9: Response Averaged Head for Cutwater and Vane Arrangement

Figure 10: Stage 1 Interaction (-1 corresponds to inline and +1 corresponds to 30 degree vane stagger)

Figure 11: Typical impeller shroud failure.

Figure 12: Axial velocity at the impeller outlet, illustrating mixing between the two sides of the double entry impeller

Tables

Location	Description	Parameter	Value
Double Entry Impeller	Inlet Eye Diameter (m)	D_1	0.177
	Average Leading Edge Blade Angle (^{o})	β_L	26
	Maximum Impeller Outlet Diameter (m)	D_2	0.366
	Average Trailing Edge Blade Angle (^{o})	β_T	22.5
	Impeller Outlet Width (m)	b_2	0.061
	Blade number (per side)	z	6
	Total Blade Wrap Angle (^{o})	θ	102
	Blade Thickness (m)	t_B	0.007
	Leading Edge Blade Radius (m)	r	0.002
Double Volute	Suction Branch Diameter (m)	D_s	0.400
	Discharge Branch Diameter (m)	D_d	0.300
	Volute Width (m)	B_3	0.105
	Radius to Cutwater (m)	R_3	0.190

Table 1: Main characteristics of pump arrangements

Experimental Arrangement	Cutwater Gap	Snubber Gap	Sidewall Clearance	Vane Arrangement
1	3.83% [-1]	0.27% [-1]	100% [+1]	0 degrees [-1]
2	3.83% [-1]	1.10% [0]	50% [0]	15 degrees [0]
3	3.83% [-1]	1.64% [+1]	25% [-1]	30 degrees [+1]
4	6.00% [0]	0.27% [-1]	50% [0]	30 degrees [+1]
5	6.00% [0]	1.10% [0]	25% [-1]	0 degrees [-1]
6	6.00% [0]	1.64% [+1]	100% [+1]	15 degrees [0]
7	7.95% [+1]	0.27% [-1]	25% [-1]	15 degrees [0]
8	7.95% [+1]	1.10% [0]	50% [0]	30 degrees [+1]
9	7.95% [+1]	1.64% [+1]	100% [+1]	0 degrees [-1]

Table 2: Geometric configuration of Taguchi arrangements

Pump Location	Arrangement 2			
	Percentage Variation		Normalised Pulsation Value ($x10^{-3}$)	
	1.00Qn	0.25Qn	1.00Qn	0.25Qn
C1	35%	12%	56	101
C3	8%	20%	56	169
C4	40%	22%	67	189
C5	27%	16%	231	315
C6	21%	27%	200	268
C8	20%	3%	81	330
C9	3%	22%	49	67
Shroud	12%	7%	128	281
Head	3.9%	6.8%	-	-

Table 3: Percentage variations for pressure pulsations and generated head with industrial experimental tests for arrangement 2

Arr.	Single Rotation Average Performance		Normalised Pressure Pulsations ($x10^{-3}$)													
			Leakage Flow Path Locations					Volute Locations					Impeller Outlet Locations			
	Head (m)	Hyd. Eff (%)	C1	C2	C10	C3	C4	C5	C6	C7	C8	C9	Blade Press. Face	Blade Suct. Face	Shroud Blade Pos.	Shroud Mid Pos.
1	36.1	85.7	94	87	94	90	101	253	259	217	167	72	411	185	181	149
2	34.7	86.7	56	43	61	56	67	231	200	134	81	49	332	254	128	115
3	35.2	87.3	38	35	37	63	95	264	208	180	119	25	381	234	178	160
4	32.7	87.4	30	30	33	38	48	172	140	122	94	22	247	189	78	73
5	33.8	86.8	89	75	89	85	109	242	203	185	143	65	327	207	206	137
6	32.9	88.3	56	45	49	40	42	133	108	79	67	40	228	167	122	114
7	30.9	88.3	50	44	45	41	42	118	96	83	74	34	175	131	75	62
8	30.3	88.6	23	19	25	27	36	134	98	83	50	15	148	126	74	68
9	31.8	86.6	72	70	73	73	77	199	153	149	113	44	206	155	129	84

Table 4: Normalised pressure pulsation ($x10^{-3}$) and pump performance results for 1.00Qn flow rate

Arr.	Single Rotation Average Performance		Normalised Pressure Pulsations (x10^{-3})													
			Leakage Flow Path Locations					Volute Locations					Impeller Outlet Locations			
	Head (m)	Hyd. Eff (%)	C1	C2	C10	C3	C4	C5	C6	C7	C8	C9	Blade Press. Face	Blade Suct. Face	Shroud Blade Pos.	Shroud Mid Pos.
1	39.3	44.1	58	63	56	83	107	233	263	340	316	86	693	444	432	540
2	39.0	42.0	38	51	42	73	94	289	221	218	185	44	628	291	228	355
3	39.0	42.0	25	29	30	63	87	225	226	204	173	36	582	319	295	364
4	37.3	39.6	42	43	42	54	64	260	210	188	159	28	526	373	217	261
5	37.9	41.5	45	50	49	89	132	308	237	287	278	68	578	333	275	359
6	37.0	39.5	33	25	26	35	50	177	136	124	154	32	423	338	197	275
7	35.7	37.7	26	26	27	29	43	159	116	140	163	36	416	347	191	279
8	36.0	37.8	24	30	29	37	45	143	124	111	109	21	421	312	196	214
9	36.3	39.3	60	55	58	68	79	223	163	186	196	49	455	297	260	252

Table 5: Normalised pressure pulsation and pump performance results for 0.50Qn flow rate

Arr.	Single Rotation Average Performance		Normalised Pressure Pulsations (x10^{-3})													
			Leakage Flow Path Locations					Volute Locations					Impeller Outlet Locations			
	Head (m)	Hyd. Eff (%)	C1	C2	C10	C3	C4	C5	C6	C7	C8	C9	Blade Press. Face	Blade Suct. Face	Shroud Blade Pos.	Shroud Mid Pos.
1	39.5	33.1	114	115	125	123	132	313	283	330	293	113	648	373	355	522
2	38.2	33.2	101	124	77	169	189	315	268	309	330	67	580	291	281	328
3	39.4	32.8	63	59	50	98	111	272	264	303	182	44	714	319	340	388
4	37.5	30.4	49	50	43	62	72	206	216	184	160	34	576	380	270	353
5	38.4	32.3	95	90	90	112	136	209	233	298	294	80	611	379	288	483
6	37.3	30.1	59	77	59	96	102	176	174	174	151	46	430	338	253	367
7	35.9	28.3	42	40	46	45	58	223	171	136	165	43	427	347	201	359
8	35.8	28.0	38	47	45	55	61	231	173	158	124	26	468	312	54	283
9	36.0	32.6	99	82	94	88	87	214	227	227	170	68	473	351	261	388

Table 6: Normalised pressure pulsation and pump performance results for 0.25Qn flow rate

Arrangement	Response Average Pressure Pulsation (Normalised)		
	-1	0	+1
Cutwater Gap	0.222	0.150	0.116
Snubber Gap	0.165	0.167	0.156
Sidewall Clearance	0.169	0.164	0.155
Vane Arrangement	0.205	0.134	0.149

Table 7: Response averages for location C6 at 1.00Qn

	Normalised Pressure Pulsations					Single Rotation Averaged Pump Performance		
	Leakage Flow Path		Volute		Impeller Outlet			
Geometric Parameter	C2	C4	C6	C9	Pressure Face	Head (m)	Power (kW)	Hyd.Eff. (%)
Cutwater	4.11	31.53	66.69	16.39	94.42	91.10	85.73	34.41
Snubber	2.43	1.62	0.73	2.76	3.45	0.72	0.68	2.10
Sidewall	0.70	13.42	1.14	0.79	0.28	0.26	0.17	10.33
Vane	92.75	53.43	31.44	80.05	1.84	7.91	13.42	53.16

Table 8 Percentage contributions for 1.00Qn flow rate at selected pump locations

	Normalised Pressure Pulsations					Single Rotation Averaged Pump Performance		
	Leakage Flow Path		Volute		Impeller Blade			
Geometric Parameter	C2	C4	C6	C9	Pressure Face	Head (m)	Power (kW)	Hyd.Eff. (%)
Cutwater	11.76	34.17	67.19	17.88	63.30	95.17	80.92	54.53
Snubber	7.64	9.67	3.55	5.08	16.35	0.50	0.22	2.65
Sidewall	21.12	7.97	3.94	2.31	6.18	0.09	0.14	0.98
Vane	59.48	48.18	25.32	74.72	14.17	4.23	18.73	41.83

Table 9 Percentage contributions for 0.50Qn flow rate at selected pump locations

	Normalised Pressure Pulsations					Single Rotation Averaged Pump Performance		
	Leakage Flow Path		Volute		Impeller Outlet			
Geometric Parameter	C2	C4	C6	C9	Pressure Face	Head (m)	Power (kW)	Hyd.Eff. (%)
Cutwater	40.02	40.03	72.92	23.59	66.37	88.91	52.41	81.62
Snubber	8.29	30.90	0.08	3.05	7.73	0.22	6.75	10.06
Sidewall	11.11	5.02	7.46	1.06	2.43	3.84	12.19	7.67
Vane	40.57	24.06	19.54	72.30	23.47	7.04	28.65	0.65

Table 10 Percentage contributions for 0.25Qn flow rate at selected pump locations

Arrangement	A (Cutwater Clearance)	B (Vane Arrangement)	AB (Interaction)	C6
1	3.83% [-1]	0 degrees [-1]	+1	0.259
3	3.83% [-1]	30 degrees [+1]	-1	0.208
9	7.95% [+1]	0 degrees [-1]	-1	0.153
8	7.95% [+1]	30 degrees [+1]	+1	0.098
			Result Total	0.718

Table 11: Stage 1 array arrangement with sample data for location C6 at 1.00Qn

		Leakage Flow		Volute		Impeller	Head
		C2	C4	C6	C9	Pressure Face	
1.00Qn							
Cutwater (A)	**-1**	0.061	0.098	0.233	0.048	0.396	35.62
	+1	0.044	0.056	0.125	0.029	0.177	31.08
	Δ/2	-0.008	-0.021	-0.054	-0.009	-0.109	-2.27
Vane Arr. (B)	**-1**	0.078	0.089	0.206	0.058	0.308	33.94
	+1	0.027	0.065	0.153	0.02	0.264	32.76
	Δ/2	-0.025	-0.012	-0.026	-0.019	-0.022	-0.587
Interaction (AB)	**-1**	0.052	0.086	0.180	0.034	0.293	33.51
	+1	0.053	0.068	0.178	0.043	0.279	33.19
	Δ/2	0.000	-0.009	-0.001	0.004	-0.007	-0.162
Grand Mean		0.052	0.077	0.180	0.039	0.287	33.35
0.25Qn							
Cutwater (A)	**-1**	0.087	0.1215	0.273	0.078	0.681	39.47
	+1	0.064	0.074	0.2	0.047	0.470	35.94
	Δ/2	-0.011	-0.024	-0.036	-0.016	-0.105	-1.76
Vane Arr. (B)	**-1**	0.098	0.109	0.255	0.090	0.560	37.79
	+1	0.053	0.086	0.218	0.035	0.591	37.62
	Δ/2	-0.023	-0.012	-0.018	-0.028	0.0152	-0.087
Interaction (AB)	**-1**	0.070	0.099	0.245	0.056	0.593	37.72
	+1	0.081	0.096	0.228	0.069	0.558	37.69
	Δ/2	0.005	-0.001	-0.008	0.007	-0.018	-0.017
Grand Mean		0.076	0.100	0.237	0.063	0.596	37.70

Table 12: Response averages, effects and half effects for stage 1 analysis at two flow rates

Arrangement	A (Cutwater Clearance)	B (Vane Arrangement)	AB (Interaction)	C6
2	3.83% [-1]	15 degrees [-1]	+1	0.200
3	3.83% [-1]	30 degrees [+1]	-1	0.208
7	7.95% [+1]	15 degrees [-1]	-1	0.096
8	7.95% [+1]	30 degrees [+1]	+1	0.098
			Result Total	0.602

Table 13: Stage 2 array arrangement with sample data for location C6 at 1.00Qn

		Leakage Flow		Volute		Impeller	Head
		C2	C4	C6	C9	Pressure Face	
1.00Qn							
Cutwater (A)	**-1**	0.039	0.081	0.204	0.037	0.356	34.95
	+1	0.031	0.039	0.097	0.024	0.161	30.61
	Δ/2	-0.004	-0.021	-0.053	-0.006	-0.097	-2.172
Vane Arr. (B)	**-1**	0.043	0.054	0.148	0.041	0.253	32.80
	+1	0.027	0.065	0.153	0.02	0.264	32.76
	Δ/2	-0.008	0.005	0.002	-0.011	0.005	-0.017
Interaction (AB)	**-1**	0.0395	0.068	0.152	0.029	0.278	33.04
	+1	0.031	0.051	0.149	0.032	0.240	32.52
	Δ/2	-0.004	-0.008	-0.001	0.001	-0.019	-0.262
Grand Mean		0.035	0.060	0.150	0.031	0.259	32.78
0.25Qn							
Cutwater (A)	**-1**	0.091	0.15	0.265	0.055	0.647	38.79
	+1	0.043	0.059	0.172	0.034	0.447	35.85
	Δ/2	-0.024	-0.045	-0.047	-0.010	-0.100	-1.47
Vane Arr. (B)	**-1**	0.082	0.123	-0.047	0.055	0.503	37.02
	+1	0.053	0.086	-0.047	0.035	0.591	37.62
	Δ/2	-0.014	-0.019	-0.001	-0.010	0.044	0.297
Interaction (AB)	**-1**	0.049	0.084	0.217	0.043	0.570	37.63
	+1	0.085	0.125	0.220	0.046	0.524	37.01
	Δ/2	0.018	0.020	0.002	0.001	-0.023	-0.307
Grand Mean		0.067	0.105	0.219	0.045	0.547	37.32

Table 14: Response averages, effects and half effects for stage 2 analysis at two flow rates

Figure 1

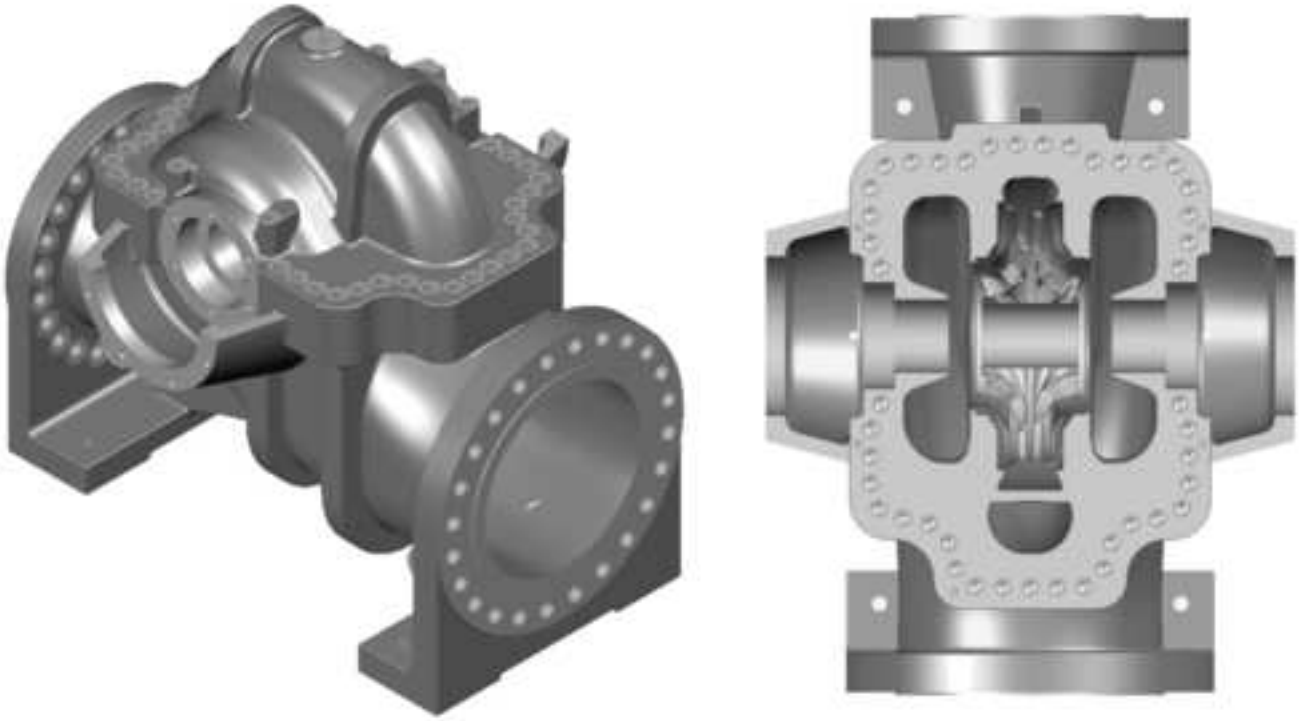

Figure 2

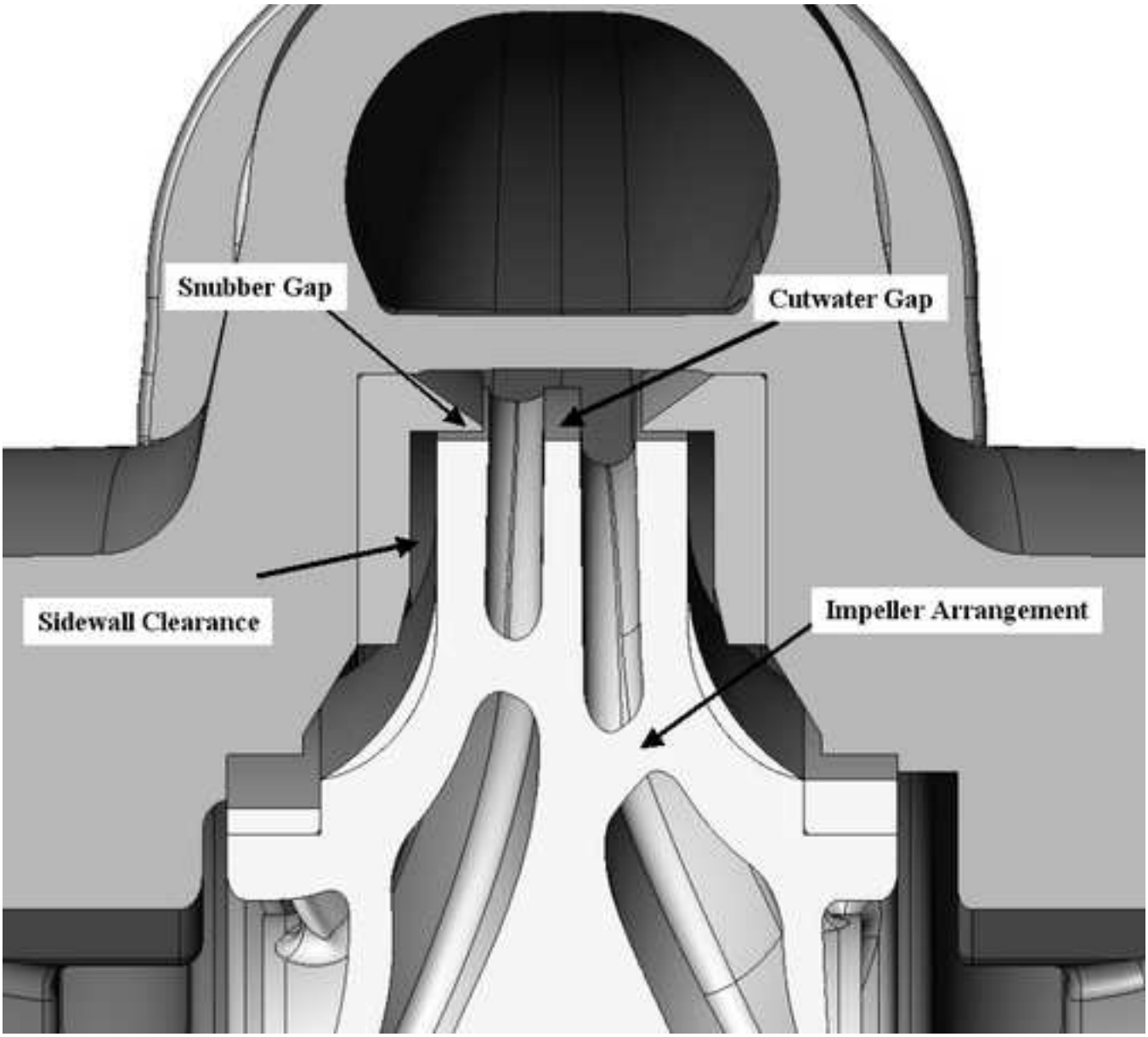

Figure 3

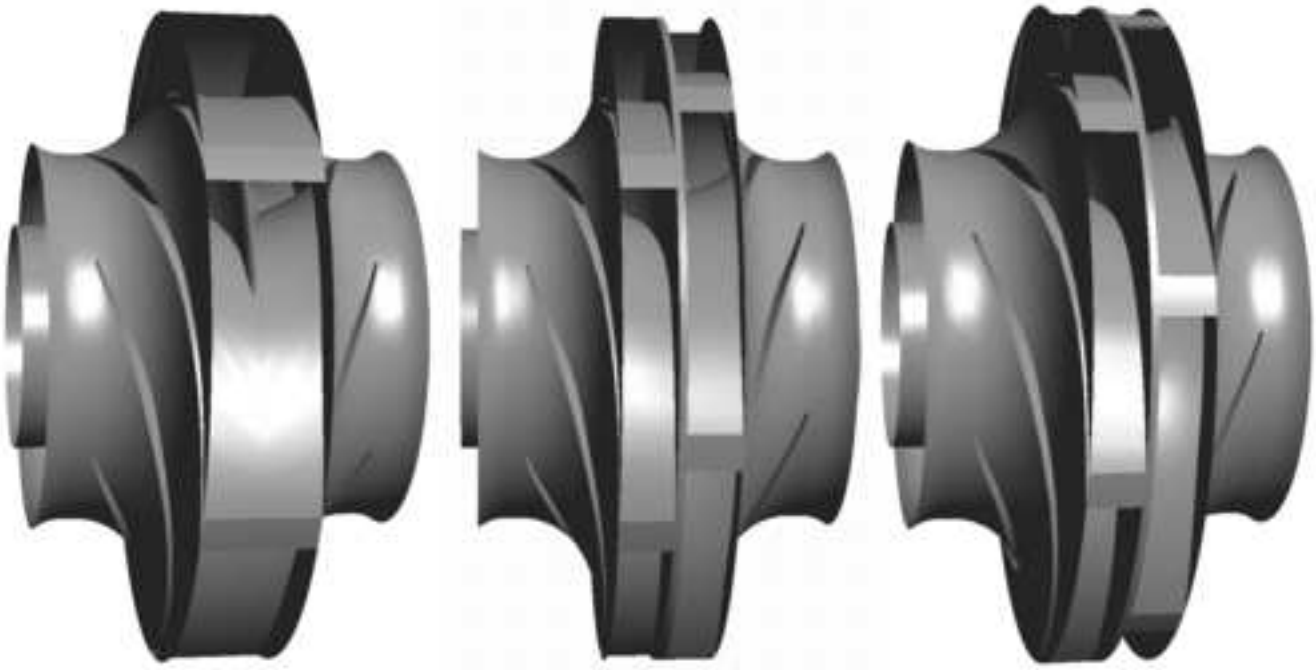

Figure 4

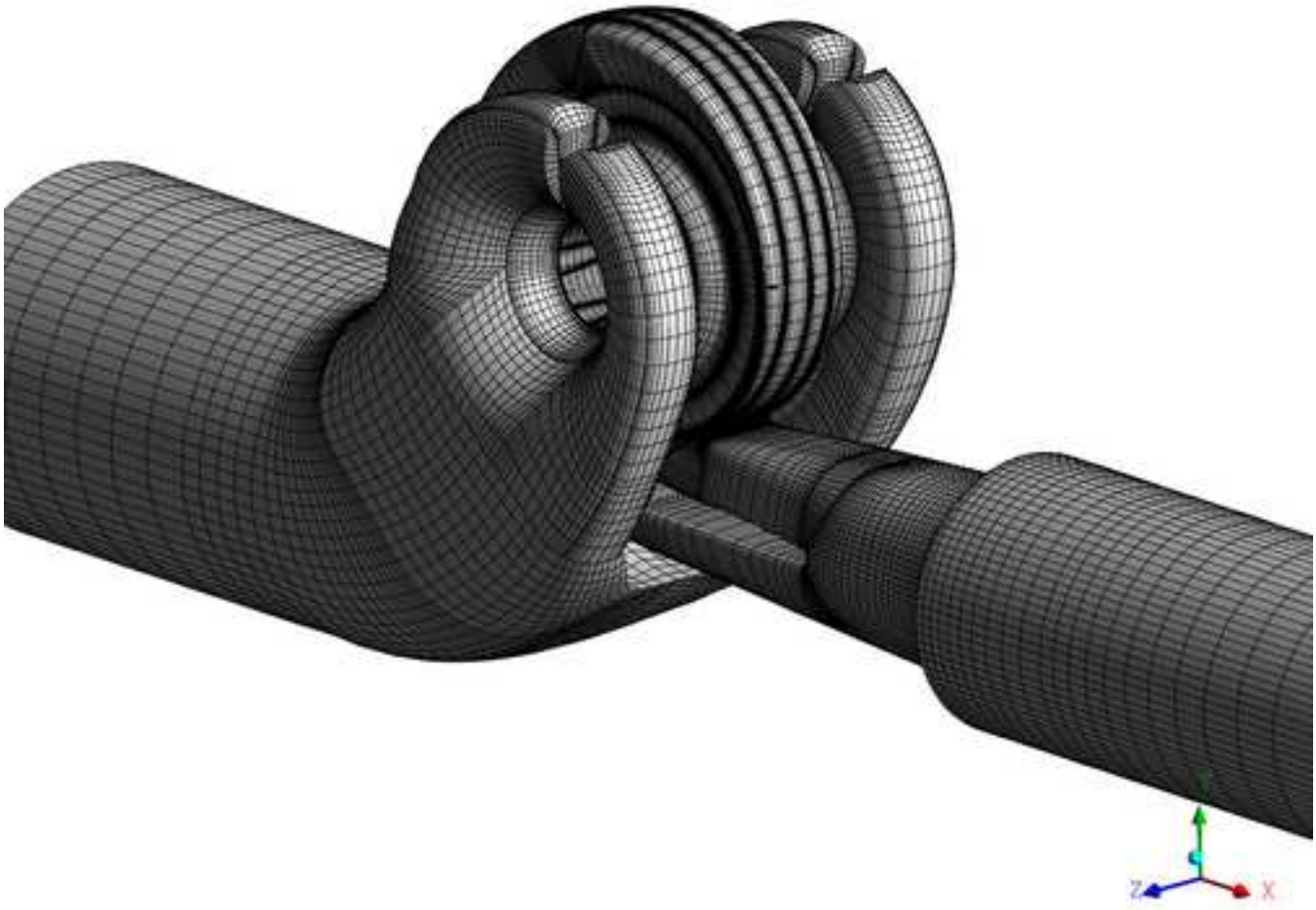

Figure 5

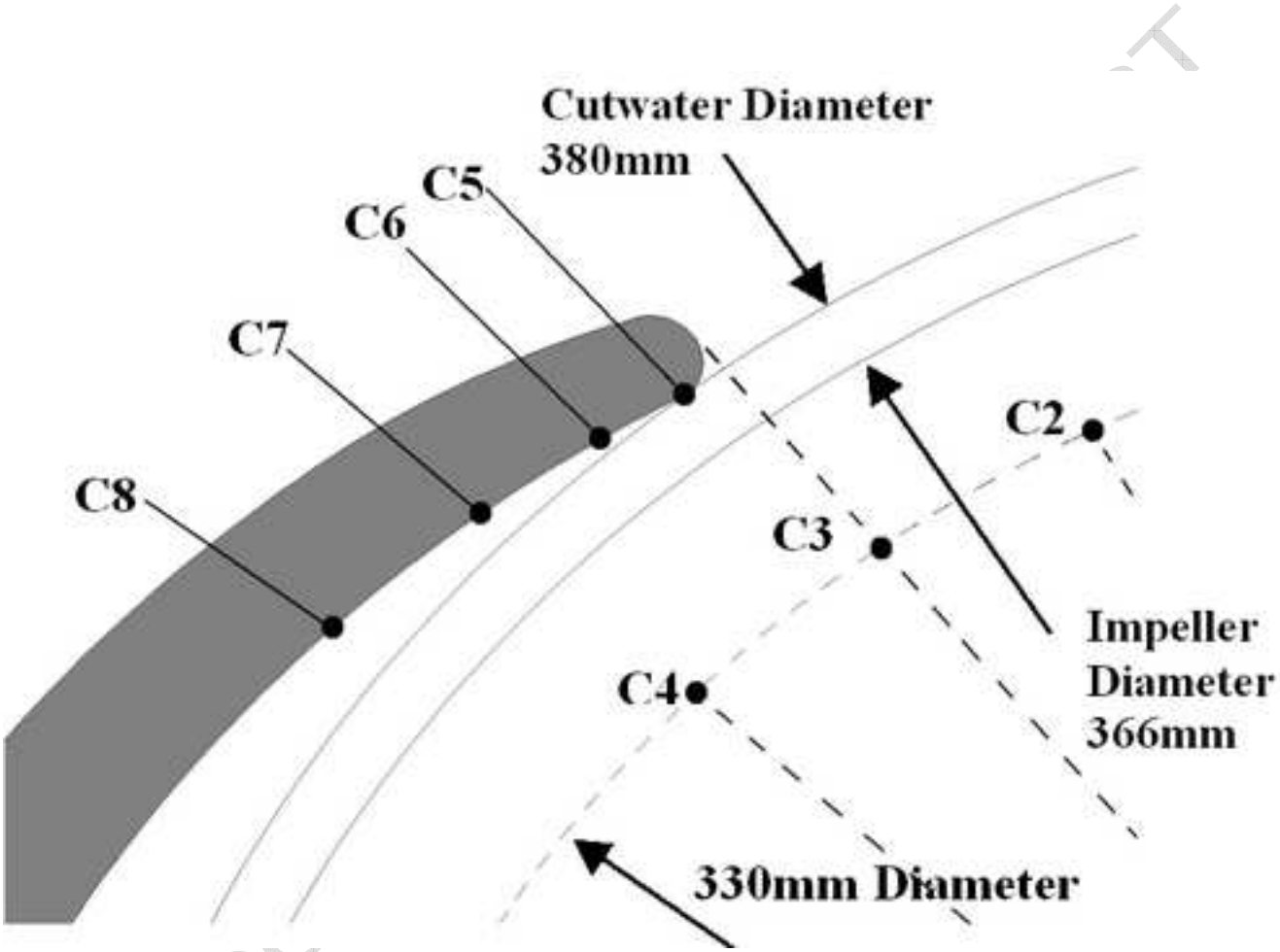

Figure 6

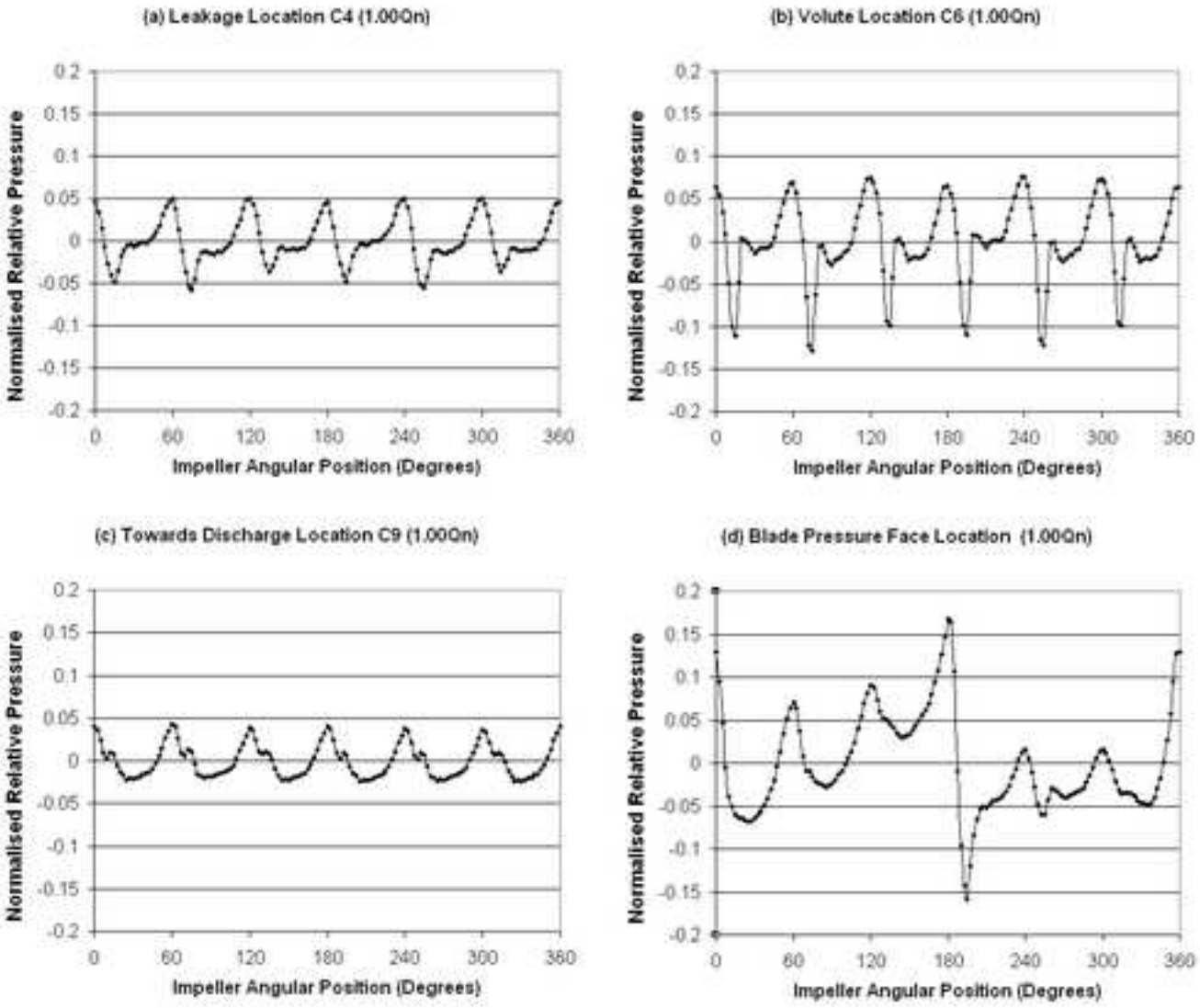

Figure 7

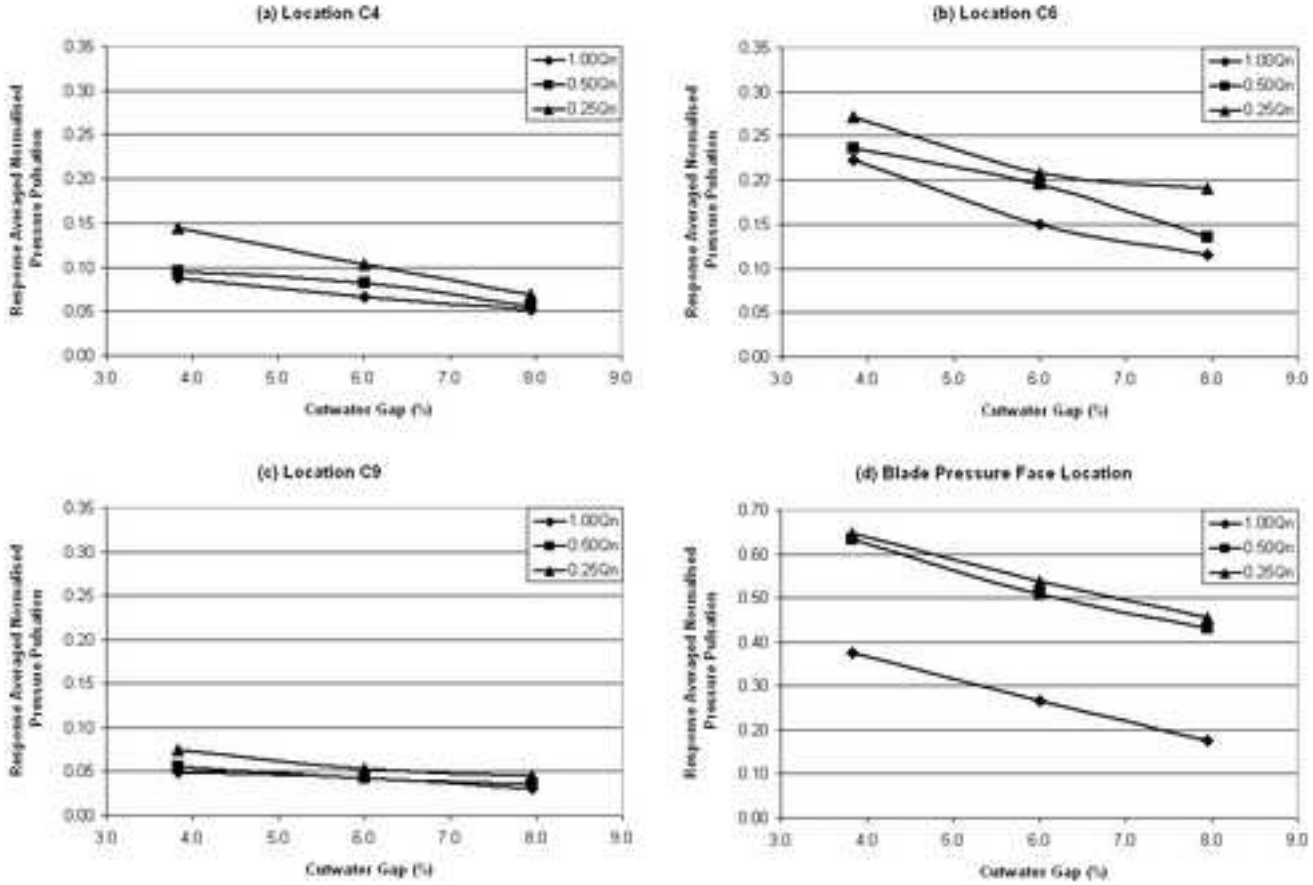

Figure 8

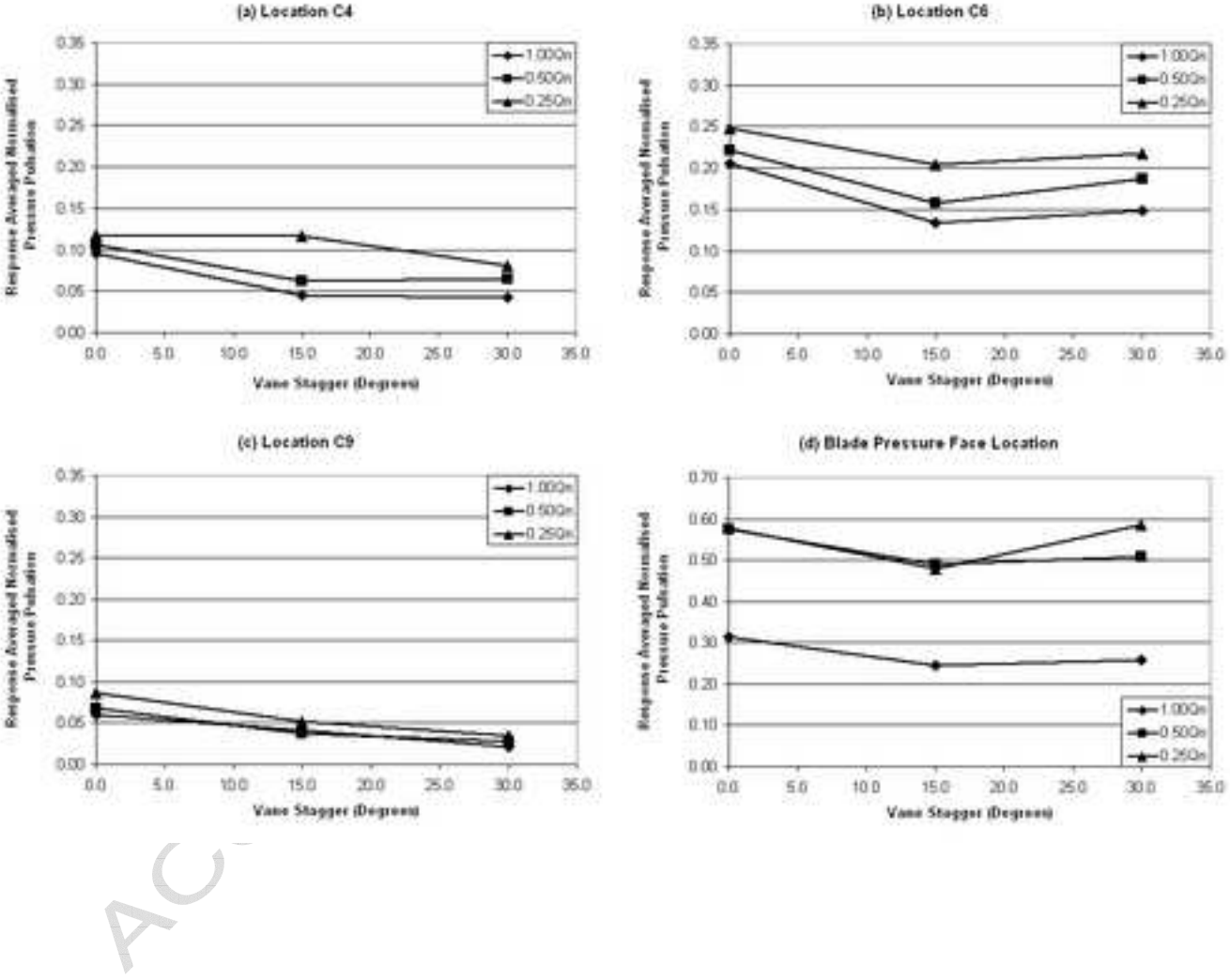

Figure 9

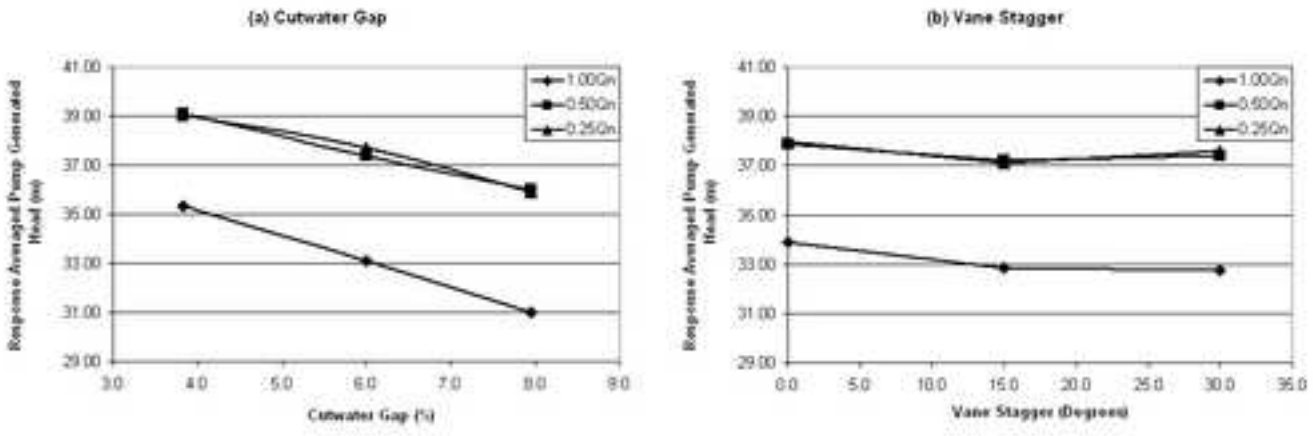

Figure 10

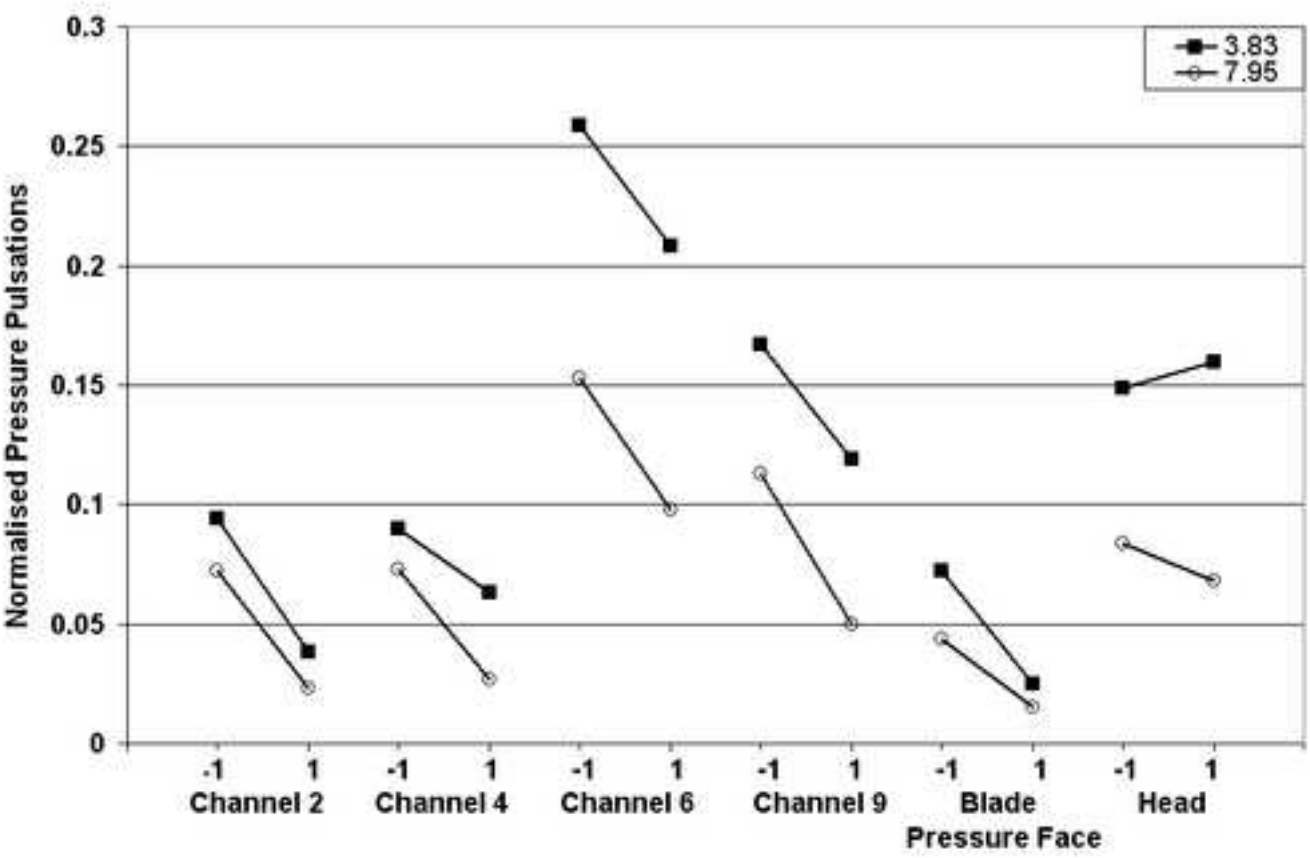

Figure 11

Figure 12

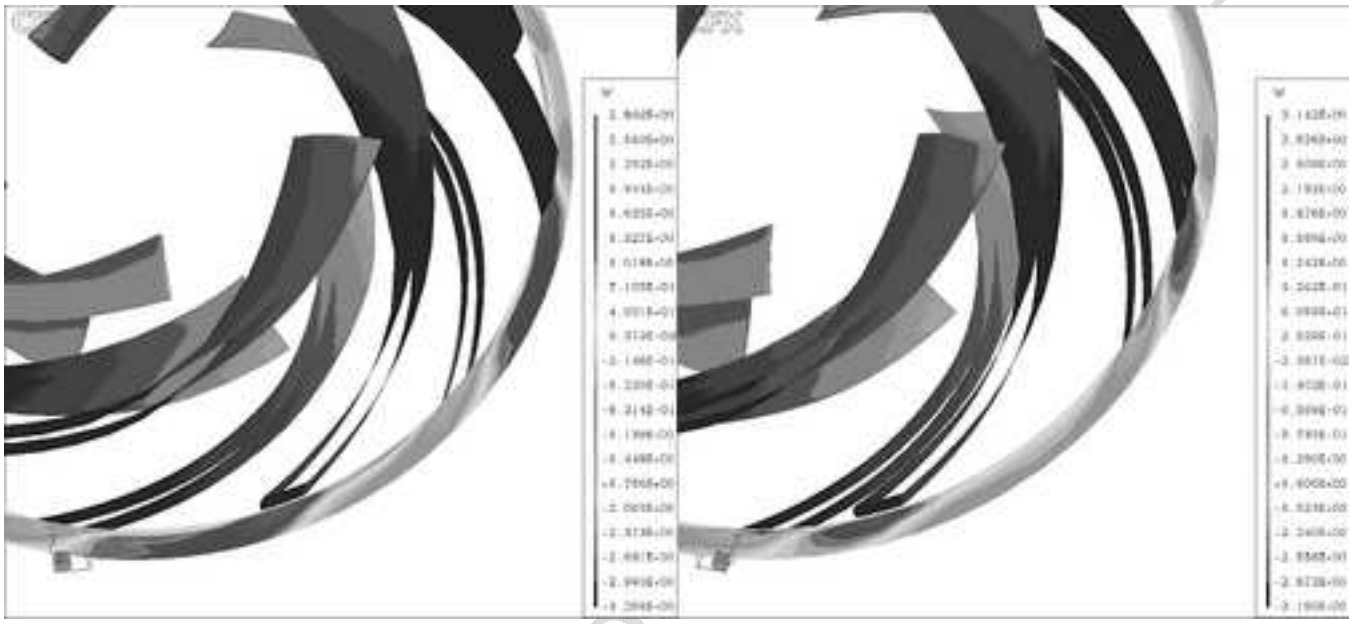

A CFD parametric study of geometrical variations on the pressure pulsations and performance characteristics of a centrifugal pump.

Spence, R.

2009-06-01T00:00:00Z

R. Spence, J. Amaral-Teixeira, A CFD parametric study of geometrical variations on the pressure pulsations and performance characteristics of a centrifugal pump, Computers & Fluids, Volume 38, Issue 6, June 2009, Pages 1243-1257

http://dx.doi.org/10.1016/j.compfluid.2008.11.013